MNHT2008-52274

GAS MICRO-FLOW MODELLING BASED ON REGULARIZED 13-MOMENT-EQUATIONS

Manuel Torrilhon[*]
Seminar for Applied Mathematics
ETH Zurich
8092 Zurich
Switzerland
Email: matorril@math.ethz.ch

Henning Struchtrup
Department of Mechanical Engineering
University of Victoria
Victoria, BC
Canada
Email: struchtr@mech.uvic.ca

ABSTRACT

We summarize our recent contributions to the development of macroscopic transport equations for gas micro-flows. A combination of the Chapman-Enskog expansion and Grad's moment method in kinetic theory of gases yields the Regularized 13-Moment-Equations (R13 equations). These equations overcome deficiencies of Grad's equations or Burnett models. They are asymptotically of super-Burnett order, i.e., of third order in the Knudsen number and linearly stable for all wave frequencies. In addition, a complete set of boundary conditions can derived from the accommodation boundary conditions of the Boltzmann equations. Mathematically, more boundary conditions are required and they can be derived from the R13 system itself through coherence relations. We present micro-channel and shock wave simulations to prove that R13 is a reliable and efficient continuum model for micro-flows of gases with moderate Knudsen numbers.

INTRODUCTION

Processes in micro-scale flows of gases or equivalently in rarefaction situations are well described by the Boltzmann equation [1] which describes the evolution of the particle distribution function in phase space, i.e. on the microscopic level.

The relevant scaling parameter to characterize processes in micro-flow gases is the Knudsen number Kn, defined as the ratio between the mean free path of a particle and a relevant length scale. If the Knudsen number is small, the Boltzmann equation can be reduced to simpler models, which allow faster solutions. Indeed, if $Kn < 0.01$ (say), the hydrodynamic equations, the laws of Navier-Stokes and Fourier (NSF), can be derived from the Boltzmann equation, e.g. by the Chapman-Enskog method [2]. The NSF equations are macroscopic equations for mass density ρ, velocity v_i and temperature T, and thus pose a mathematically less complex problem than the Boltzmann equation.

Macroscopic equations for rarefied gas flows at Knudsen numbers above 0.01 promise to replace the Boltzmann equation with simpler equations that still capture the relevant physics. The Chapman-Enskog expansion is the classical method to achieve this goal, but the resulting Burnett and super-Burnett equations are unstable [3]. To fix these problems in the framework of Chapman-Enskog expansion is cumbersome [4,5]. Nevertheless, in some cases Burnett equations could be used for simulations of non-equilibrium gases [6,7].

A classical alternative is Grad's moment method [8] which extends the set of variables by adding deviatoric stress tensor σ_{ij}, heat flux q_i, and possibly higher moments of the velocity distribution function (phase density) of the particles. The resulting equations are stable but lead to spurious discontinuities in shocks [9]. Nevertheless, some successes have been obtained with moment methods and popularity is raising, see [10–14]. However, for a given value of the Knudsen number it is not clear what set of moments one would have to consider [2].

Struchtrup and Torrilhon combined both approaches by performing a Chapman-Enskog expansion around a non-equilibrium

---

[*]Address all correspondence to this author.

phase density of Grad type [15, 16] which resulted in the "Regularized 13 moment equations" (R13 equations) which form a stable set of equations for the 13 variables $(\rho, v_i, T, \sigma_{ij}, q_i)$ of super-Burnett order, i.e., of third order in the Knudsen number when asymptotically expanded. The next Section gives a review of this original derivation. An alternative approach to the problem was presented by Struchtrup in [17, 18], partly based on earlier work by Müller et al. [19]. This Order-of-Magnitude-Method is based on a rigorous asymptotic analysis of the infinite hierarchy of the moment equations. A brief outline is also given in the next Section.

One of the biggest problems for all models beyond NSF is to prescribe suitable boundary conditions for the extended equations, which should follow from the boundary conditions for the Boltzmann equation. This task was recently tackled in [20], and the general solution to the problem [21] will be discussed after the derivation of the equations, when we present boundary conditions for the R13 equations.

The second part of the paper will survey the properties of the R13 equations, which are linearly stable, obey an H-theorem for the linear case, contain the Burnett and super-Burnett equations asymptotically, predict phase speeds and damping of ultrasound waves in excellent agreement to experiments, yield smooth and accurate shock structures for all Mach numbers, and exhibit Knudsen boundary layers and the Knudsen minimum of channel flow in excellent agreement to DSMC simulations. The paper reviews detailed informations about the performance of R13 for Poiseuille flow in micro-channels and normal shock wave profiles.

The interested reader is referred to the cited literature, including the monograph [2].

DERIVATION OF R13

The derivation of the regularized 13-moment-equations has been done in two ways. Both ways give specific insight into the structure and properties of the theory.

Based on a Pseudo-Equilibrium

The original derivation [15] develops an enhanced constitutive theory for Grad's moment equations. The closure procedure of Grad is too rigid and needs to be relaxed. The new theory can be summarized in three steps

1. Identify the set of variables U and higher moments V that need a constitutive relation in Grad's theory.
2. Formulate evolution equations for the difference $R = V - V^{(\text{Grad})}(U)$ of the constitutive moments and their Grad relation.
3. Perform an asymptotic expansion of R alone while fixing *all* variables U of Grad's theory.

This procedure can in principle be performed on any system obtained by Grad's moment method, i.e., any number of moments can be considered as basic set of variables. For the derivation of R13 the first 13 moments density, velocity, temperature, stress deviator and heat flux have been considered in accordance with the classical 13-moment-case of Grad.

In the classical Grad approach the difference R is considered to be zero: All constitutive moments follow from lower moments by means of Grad's distribution $V = V^{(\text{Grad})}(U)$. This rigidity causes hyperbolicity but also artifacts like subshocks and poor accuracy. However, the evolution equation for R is in general not an identity. Instead it describes possible deviations of Grad's closure. The constitutive theory of R13 takes these deviations into account.

The evolution equation for R can not be solved exactly because it is influenced by even higher moments. Hence, an approximation is found by asymptotic expansion. In doing this, step 3 requires a modeling assumption about a scaling cascade of the higher order moments. In the asymptotic expansion of R we fix lower moments like density and temperature but also non-equilibrium quantities like stress and heat flux. The assumption is that the higher moments R follow a faster relaxation or bear a smaller scale of significance. The expansion can be considered as an expansion around a non-equilibrium (pseudo-equilibrium).

The result for R after one expansion step is a relation that couples R to gradients of the variables U, in R13 these are gradients of stress and heat flux. The gradient terms enter the divergences in the equations for stress and heat flux and produce dissipative second order derivatives. The final system is a regularization of Grad's 13-moment-equations. The procedure resembles the derivation of the NSF-system. Indeed the NSF equations can be considered as regularization of Euler equations (i.e., Grad's 5-moment-system).

Based on Order of Magnitude

The Order-of-Magnitude-Method [17, 18] considers the infinite system of moment equations resulting from Boltzmann's equation. It does not depend on Grad's closure relations and does not directly utilize the result of asymptotic expansions. The method finds the proper equations with order of accuracy λ_0 in the Knudsen number by the following three steps:

1. Determination of the order of magnitude λ of the moments.
2. Construction of moment set with minimum number of moments at order λ.
3. Deletion of all terms in all equations that would lead only to contributions of orders $\lambda > \lambda_0$ in the conservation laws for energy and momentum.

Step 1 is based on a Chapman-Enskog expansion where a moment φ is expanded according to $\varphi = \varphi_0 + Kn\,\varphi_1 + Kn^2\varphi_2 + ...$, and the leading order of φ is determined by inserting this

ansatz into the complete set of moment equations. A moment is said to be of leading order λ if $\lambda_\beta = 0$ for all $\beta < \lambda$. This first step agrees with the ideas of [19]. Alternatively, the order of magnitude of the moments can be found from the principle that a single term in an equation cannot be larger in size by one or several orders of magnitude than all other terms [22].

In Step 2, new variables are introduced by linear combination of the moments originally chosen. The new variables are constructed such that the number of moments at a given order λ is minimal. This step gives an unambiguous set of moments at order λ.

Step 3 follows from the definition of the order of accuracy λ_0: A set of equations is said to be accurate of order λ_0, when stress and heat flux are known within the order $O\left(Kn^0\right)$.

The order of magnitude method gives the Euler and NSF equations at zeroth and first order, and thus agrees with the Chapman-Enskog method in the lower orders [17]. The second order equations turn out to be Grad's 13 moment equations for Maxwell molecules [17], and a generalization of these for molecules that interact with power potentials [2, 18]. At third order, the method was only performed for Maxwell molecules, where it yields the R13 equations [17]. It follows that R13 satisfies some optimality when processes are to be described with third order accuracy.

Result

Here, we display the original R13 equations from [15] which are build from the general conservation laws for a mon-atomic gas with mass density ρ, velocity v_i, and the temperature θ in energy units,

$$\frac{\partial \rho}{\partial t} + \frac{\partial \rho v_k}{\partial x_k} = 0, \tag{1}$$

$$\rho \frac{\partial v_i}{\partial t} + \rho v_k \frac{\partial v_i}{\partial x_k} + \frac{\partial p}{\partial x_i} + \frac{\partial \sigma_{ik}}{\partial x_k} = 0 \tag{2}$$

$$\frac{3}{2}\rho \frac{\partial \theta}{\partial t} + \frac{3}{2}\rho v_k \frac{\partial \theta}{\partial x_k} + \frac{\partial q_k}{\partial x_k} + (p\delta_{ij} + \sigma_{ij})\frac{\partial v_i}{\partial x_j} = 0 \tag{3}$$

where δ_{ij} is the Kronecker symbol or identity matrix. For the pressure p we assume the ideal gas law $p = \rho\theta$. We use cartesean index notation with $i,j,k,l \in \{1,2,3\}$ and summation convention. The additional evolution equations that closes the system are given by

$$\frac{\partial \sigma_{ij}}{\partial t} + \frac{\partial \sigma_{ij} v_k}{\partial x_k} + \frac{4}{5}\frac{\partial q_{\langle i}}{\partial x_{j\rangle}} + 2p\frac{\partial v_{\langle i}}{\partial x_{j\rangle}}$$
$$+ 2\sigma_{k\langle i}\frac{\partial v_{j\rangle}}{\partial x_k} + \frac{\partial m_{ijk}}{\partial x_k} = -\frac{p}{\mu}\sigma_{ij} \tag{4}$$

for the stress deviator σ_{ij} and

$$\frac{\partial q_i}{\partial t} + \frac{\partial q_i v_k}{\partial x_k} + p\frac{\partial(\sigma_{ik}/\rho)}{\partial x_k} + \frac{5}{2}(p\delta_{ik} + \sigma_{ik})\frac{\partial \theta}{\partial x_k} - \frac{\sigma_{ij}}{\rho}\frac{\partial \sigma_{jk}}{\partial x_k}$$
$$+ (m_{ijk} + \frac{6}{5}q_{\langle i}\delta_{jk\rangle} + q_k\delta_{ij})\frac{\partial v_j}{\partial x_k} + \frac{1}{2}\frac{\partial \hat{R}_{ik}}{\partial x_k} = -\frac{2p}{3\mu}q_i \tag{5}$$

the heat flux q_i with μ the viscosity of the gas. Angular brackets around indices denote the symmetric deviatoric part, e.g., $A_{\langle ij\rangle} = \frac{1}{2}(A_{ij} + A_{ji}) - \frac{1}{3}A_{kk}\delta_{ij}$ and analogously for three indices, see [2]. The remaining quantities m_{ijk} and $\hat{R}_{ij}$ represent higher moments. These are zero in the Grad case, but the R13 theory provides the gradient expressions

$$m_{ijk} = -2\mu\frac{\partial(\sigma_{\langle ij}/\rho)}{\partial x_{k\rangle}} + \frac{8}{10p}q_{\langle i}\sigma_{jk\rangle}^{(\text{NSF})} , \tag{6}$$

$$R_{ij} = -\frac{24}{5}\mu\frac{\partial(q_{\langle j}/\rho)}{\partial x_{j\rangle}} + \frac{32}{25p}q_{\langle i}q_{j\rangle}^{(\text{NSF})} + \frac{24}{7\rho}\sigma_{k\langle i}\sigma_{j\rangle k}^{(\text{NSF})} , \tag{7}$$

$$R = -12\mu\frac{\partial(q_k/\rho)}{\partial x_k} + \frac{8}{p}q_k q_k^{(\text{NSF})} + \frac{6}{\rho}\sigma_{ij}\sigma_{ij}^{(\text{NSF})} . \tag{8}$$

with $\hat{R}_{ij} = R_{ij} + \frac{1}{3}R\delta_{ij}$ and the abbreviations

$$\sigma_{ij}^{(\text{NSF})} = -2\mu\frac{\partial v_{\langle i}}{\partial x_{j\rangle}}, \qquad q_i^{(\text{NSF})} = -\frac{15}{4}\mu\frac{\partial \theta}{\partial x_i}. \tag{9}$$

In total the R13 system is given by non-linear parabolic-hyperbolic partial differential equations with relaxation. In that sense it resembles the mathematical structure of the NSF equations.

BOUNDARY CONDITIONS FOR R13

The computation of boundary conditions for the R13 equations is based on Maxwell's model for boundary conditions for the Boltzmann equation [1,2,23], which states that a fraction χ of the particles hitting the wall is thermalized, while the remaining $1 - \chi$ particles are specularly reflected. Boundary conditions for moments follow by taking moments of the boundary conditions of the Boltzmann equation. To produce meaningful boundary conditions, one needs to obey the following rules:

1. *Continuity*: In order to have meaningful boundary conditions for all accommodation coefficients $\chi \in [0,1]$, only boundary conditions for tensors with an odd number of normal components should be considered [20, 21].
2. *Consistency*: Only boundary conditions for fluxes that actually appear in the equations should be considered [21].

3. *Coherence*: The same number of boundary conditions should be prescribed for the linearized and the non-linear equations [21].

The application of Rules 1 and 2 is straight forward and yields the following set of kinetic boundary conditions (*t* and *n* denote tangential and normal tensor components, respectively) for moments

$$\sigma_{tn} = -\beta \left(PV_t + \tfrac{1}{2}m_{tnn} + \tfrac{1}{5}q_t \right) \tag{10}$$
$$q_n = -\beta \left(2P\Delta\theta + \tfrac{5}{28}R_{nn} + \tfrac{1}{15}R + \tfrac{1}{2}\theta\sigma_{nn} - \tfrac{1}{2}PV_t^2 \right)$$
$$R_{tn} = \beta \left(P\theta V_t - \tfrac{1}{2}\theta m_{tnn} - \tfrac{11}{5}\theta q_t - PV_t^3 + 6P\Delta\theta V_t \right)$$
$$m_{nnn} = \beta \left(\tfrac{2}{5}P\Delta\theta - \tfrac{1}{14}R_{nn} + \tfrac{1}{75}R - \tfrac{7}{5}\theta\sigma_{nn} - \tfrac{3}{5}PV_t^2 \right)$$
$$m_{ttn} = -\tfrac{m_{nnn}}{2} - \beta \left(\tfrac{1}{14}(R_{tt} + \tfrac{R_{nn}}{2}) + \theta(\sigma_{tt} + \tfrac{\sigma_{nn}}{2}) - PV_t^2 \right)$$

where $\Delta\theta = \theta - \theta_W$, $V_t = v_t - v_t^W$ and

$$P := \rho\theta + \frac{\sigma_{nn}}{2} - \frac{R_{nn}}{28\theta} - \frac{R}{120\theta}. \tag{11}$$

The properties of the wall are given by its temperature θ_W and velocity v_t^W and the modified accommodation coefficient

$$\beta = \chi/(2-\chi)\sqrt{2/(\pi\theta)}. \tag{12}$$

In extrapolation of the theory of accommodation these coefficients that occur in every equation of (10) could be chosen differently. This represents a different accommodation of the single moment fluxes, like shear or heat flux, see [21].

The first condition above is the slip condition for the velocity, while the second equation is the jump condition for the temperature. In a manner of speaking, the other conditions can be described as jump conditions for higher moments.

When the R13 equations are considered for channel flows in their original form, it turns out that a different number of boundary conditions is required to solve the fully non-linear and the linearized equations. Since this would not allow a smooth transition between linear and non-linear situations, we formulated the third rule as given above.

Asymptotic analysis shows that some terms can be changed without changing the overall asymptotic accuracy of the R13 equations. This leads to the algebraization of several non-linear terms in the pde's which, after some algebra, leads to algebraic relations, termed as bulk equations, between the moments which serve as additional boundary conditions for the non-linear equa-

tions [21],

$$\hat{R}_{nn} = \frac{136}{25p}q_n^2 - \frac{72}{35\rho}\sigma_{tn}^2, \tag{13}$$
$$m_{tnn} = \frac{32}{45p}\sigma_{tn}q_n. \tag{14}$$

These equations have a special interpretation. The possibility to prescribe kinetic boundary conditions like in (10) for moments is related to the ability of the moments to produce a, so-called Knudsen layer. The Knudsen layer is a boundary layer that occurs close to wall in high Knudsen number flows like in micro channels. The kinetic boundary condition specifies the amplitude of the boundary layer. In the R13-system some variables, like parallel heat flux and normal stresses, are able to produce a Knudsen layer, while others, like the higher moments $\hat{R}_{nn}$ and m_{tnn}, can not. This is due to the finite number of moments considered. In the infinite moment hierarchy all moments exhibit Knudsen layers, see [24].

Due to the lack of a Knudsen layer, kinetic boundary conditions may not be used for the moments $\hat{R}_{nn}$ and m_{tnn}. Instead, we assume that the boundary layer is relaxed infinitely fast to an interior solution - the bulk solution given in (13). Hence, the bulk solution turns out to be the natural boundary conditions for Knudsen-layer-less variables. Details of this interpretation can be found in [21].

COMPUTATIONS AND SIMULATIONS

We summarize the most important features of the R13 equations which result from analytical considerations and from analytical and numerical solutions. The results of R13 have been compared to experimental data as well as to direct simulation results obtained by DSMC [25].

The R13 equations:

▶ are derived in a rational manner by means of the order of magnitude method [17, 18], or from a Chapman-Enskog expansion around non-equilibrium [15, 16],
▶ are of third order in the Knudsen number [2, 15–18],
▶ are linearly stable for initial and boundary value problems [15, 16],
▶ contain Burnett and super-Burnett asymptotically in the linear [15] and non-linear [16] case,
▶ predict phase speeds and damping of ultrasound waves in excellent agreement to experiments [15],
▶ give smooth shock structures for all Mach numbers, with good agreement to DSMC simulations for $Ma \lesssim 3$ (see below) [16],
▶ are accompanied by a complete set of boundary conditions [21],

- ▶ obey an H-theorem for the linear case, including the boundaries [26],
- ▶ exhibit the Knudsen paradox for channel flows (see next section) [21, 26],
- ▶ exhibit Knudsen boundary layers in good agreement to DSMC [27, 28],
- ▶ are accessible to numerical simulations in multiple space dimensions [29],
- ▶ predict light scattering spectra in accordance to experiments [30]

We proceed with reviewing the results for shock waves and micro-channel flows.

Micro-Channel Flows

To approach micro-channel flows we study a special class of steady shear flows that include steady Couette or Poiseuille flows. For the R13 system, shear flow is a multi-dimensional phenomenon in the sense that it produces a fully multi-dimensional reaction for the stress tensor and heat flux. Introducing $x_i \hat{=} (x,y,z)$, we consider shear flow which is homogeneous in z-direction and define the remaining non-vanishing parts of stress tensor and heat flux as

$$\sigma = \begin{pmatrix} \sigma_{xx} & \sigma_{xy} & 0 \\ \sigma_{yx} & \sigma_{yy} & 0 \\ 0 & 0 & \sigma_{zz} \end{pmatrix}, \quad \mathbf{q} = (q_x, q_y, 0) \quad (15)$$

where $\sigma_{xy} = \sigma_{yx}$, and $\sigma_{zz} = -(\sigma_{xx} + \sigma_{yy})$ since σ must be trace-free. For the velocity we assume $v_y = v_z = 0$ and

$$\mathbf{v}(x,y,z) = (v_x(y), 0, 0). \quad (16)$$

The force acts only in x-direction, $\mathbf{f} = (F,0,0)$. This setting is valid for channel flows as displayed in Fig. 1. The gas is confined between two infinite plates at distance L and is moving solely in x-direction. The walls are moving with x-velocities $v_W^{(0,1)}$ and may be heated with different temperatures $\theta_W^{(0,1)}$.

In this setting we have 8 independent variables in the R13 equations, namely $\{\rho, v_x, p, \sigma_{xx}, \sigma_{yy}, \sigma_{xy}, q_x, q_y\}$. Optionally, the pressure p can be replaced by the temperature θ. The 5 remaining relevant constitutive quantities are $\{m_{xxy}, m_{xyy}, m_{yyy}, \hat{R}_{xy}, \hat{R}_{yy}\}$. The system (1)-(9) reduces to 13 first order non-linear ordinary differential equations in the space variable y. The equations uncover a striking simplicity by decomposing into three linearly decoupled blocks. The coupling is displayed by writing the vector of variables in the form

$$\mathbf{U} = \{v_x, \sigma_{xy}, q_x, m_{xyy}, R_{xy} \,|\, \theta, q_y, \sigma_{yy}, \hat{R}_{yy}, m_{yyy} \,|\, \rho, \sigma_{xx}, m_{xxy}\} \quad (17)$$
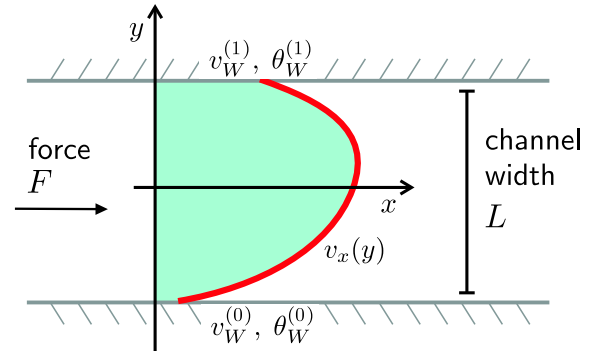

Figure 1. General setting for shear flow between two infinite plates. The plates are moving and maybe heated.
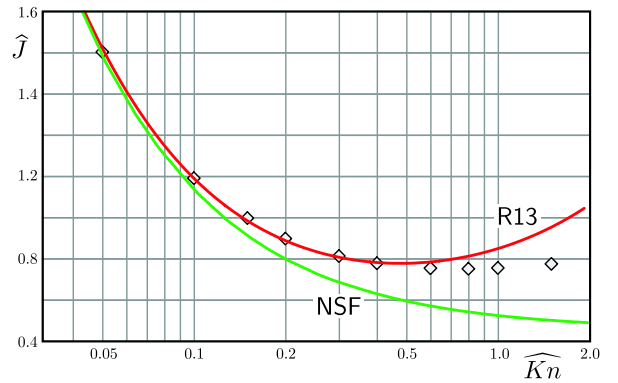

Figure 2. Averaged mass flow rate in acceleration-driven channel flow. The R13-equations predict the Knudsen paradox.

The first block describes the velocity part with the balances of v_x, σ_{xy}, and q_x, and higher moments m_{xyy} and $\hat{R}_{xy}$, the second block describes the temperature part with balances of θ, q_y, and σ_{yy}, and higher moments $\hat{R}_{yy}$ and m_{yyy}. Both parts are governed dominantly by two classical variables, (v_x, σ_{xy}) and (θ, q_y), respectively, which behave essentially in an intuitive way. In NSF the second variable is related to the gradient of the first. The third variable in both parts, q_x and σ_{yy}, respectively, is given by a seemingly classical variable which however plays a non-intuitive role. It represents a *heat flux produced by a velocity shear* in the first block and a *normal stress due to temperature difference* in the second. Both are typical bulk effects in micro-flows of gases. Through these variables the classical variables velocity and temperature are coupled to the high order internal quantities, m_{xyy} and $\hat{R}_{xy}$, and, $\hat{R}_{yy}$ and m_{yyy}, respectively. From tensorial considerations the first block can be identified with mixed normal/tangential variables (shear), while the second block couples the purely normal variables (temperature). The last block combines the density and purely tangential tensorial variables and
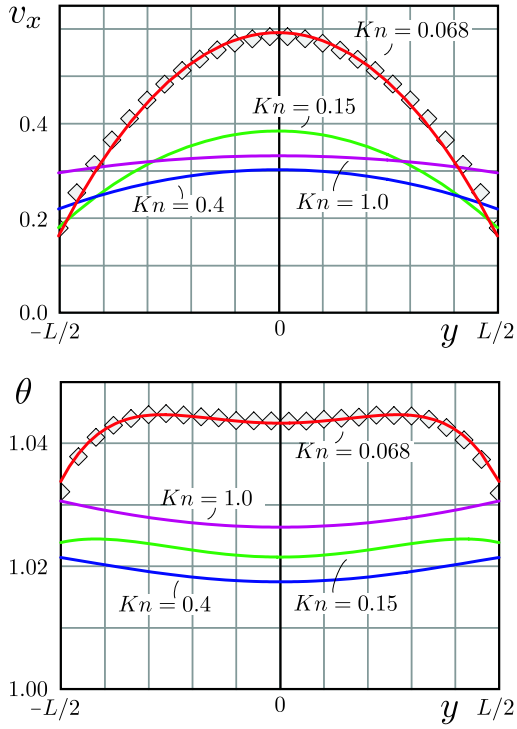
Figure 3. Velocity and temperature profiles in acceleration driven channel flow for various Knudsen numbers. The symbols in the case $Kn = 0.068$ represent a DSMC result.

Figure 4. Micro-scale effects, like parallel heat flux q_x and normal stresses σ_{yy}, in micro-channels as predicted by R13 for various Knudsen numbers. The symbols in the case $Kn = 0.068$ represent a DSMC result.

exhibits only a minor influence.

In this paper we consider Poiseuille flow given by acceleration-driven channel flow with walls at rest and identical temperatures. The channel is considered to be infinitely long such that a full velocity profile has developed from the viscous boundary layers. The given acceleration can be interpreted as a homogeneous pressure gradient. The Knudsen number

$$Kn = \frac{L}{\lambda} \qquad (18)$$

with mean free path $\lambda = \mu/(\rho \sqrt{\theta})$ is based on the width of the channel.

Gas flow through a channel is known to exhibit a paradoxical behavior known as Knudsen paradox, [33]. When reducing the Knudsen number in the experiment the normalized mass flow rate

$$J = \int_{-1/2}^{1/2} v(y) \, dy \qquad (19)$$

through the channel reaches a minimum and afterwards starts to increase for larger Knudsen numbers. Intuitively one would ex-
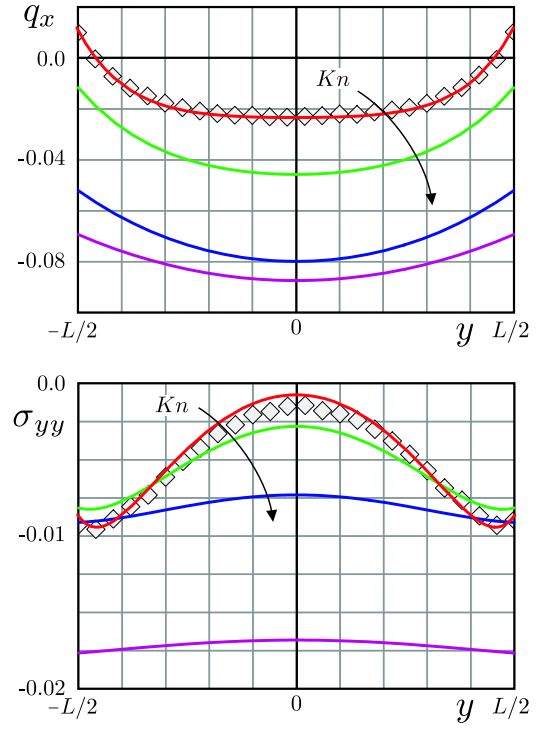
pect a decreasing mass flow for a smaller channel, but at a certain micro-scale the friction inside the gas becomes so small that the growing slip velocity at the wall dominates the mass flow.

We solve the R13-system in the form (1)-(9) for this setting with kinetic boundary conditions (10)/(13) for various Knudsen numbers. Fig. 2 shows the dimensionless mass flow rate obtained from R13 as a function of Kn. The curve clearly shows a minimum and thus correctly predicts a Knudsen paradox. The figure also shows the mass flow rate obtained with NSF and standard slip boundary conditions which clearly fails to produce a Knudsen minimum. In [34] the mass flow rate has been calculated based on the linearized Boltzmann equation and those results are given in Fig. 2 as symbols. The mass flow for R13 follows the Boltzmann result fairly accurate until $Kn \lesssim 1.0$ and then lifts off too quickly. At these high Knudsen numbers the assumptions of the theory are not valid anymore.

The mass flow rate is only a rough property of micro flows and the R13 result gives much more inside when considering the fields of the moments. Figs. 3 and 4 display some fields obtained by R13 for Knudsen numbers $Kn = 0.068, 0.15, 0.4, 1.0$. The figures show the conservation variables velocity v_x and temperature θ, as well as the micro-scale variables tangential heat flux
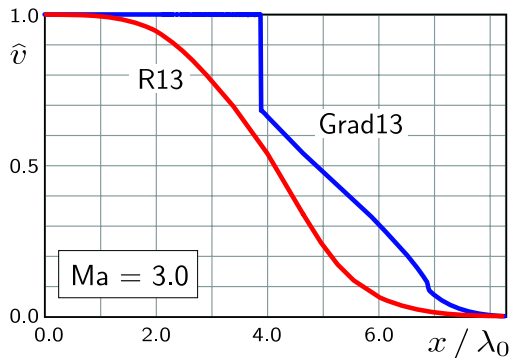
Figure 5. Comparison of a shock profile produced by R13 with the corresponding profile of Grad's equations. The regularization eliminates the sub-shock.

q_x and normal stress σ_{yy}. Note, that the channel flow produces a significant parallel heat flux q_x even though the temperature is homogenous along x. Similarly, the temperature field triggers a normal stress even though $\partial_y v_y = 0$. This is a micro-scale effect. Higher Knudsen numbers show stronger non-equilibrium as indicated by larger magnitudes of q_x and σ_{yy}. Interestingly, the temperature profile starts to invert for higher Knudsen numbers. Note also, that the Knudsen paradox can be observed in the results of the R13-system in Fig. 3. The velocity profile becomes flatter, but the slip increases and the velocity curve for $Kn = 1.0$ lies above the curve of $Kn = 0.4$.

The simulations were obtained with a dimensionless acceleration force fixed at $F = 0.23$, such that Knudsen number $Kn = 0.068$ corresponds to the case of Poiseuille flow calculated in [31] (see also [32]) by DSMC. These results are shown in Figs. 3 and 4 as symbols. R13 gives good agreement with the DSMC result.

Shock Wave Profiles

Shock waves represent a classical test case to investigate the accuracy of non-equilibrium continuum models. A shock wave travels with super-sonic speed measured in terms of the sound speed c by the Mach number $Ma = v/c$. It connects two regions of equilibrium through a rapid transition zone with a thickness of a few mean free pathes. Inside this transition strong dissipation takes place on a microscopic scale and the fields of density and temperature form smooth profiles. Classical fluid models, like Navier-Stokes-Fourier, fail to predict the profile of shock correctly even for small Mach numbers $Ma \approx 1.2$.

Shock waves are not considered as typical micro-flows especially due to the high speed behavior. However, microscopic or large Knudsen number phenomena play a major role. Also, nonlinear effects are dominant. We propose that any serious model for gas micro-flows should be tested on shock waves at least for
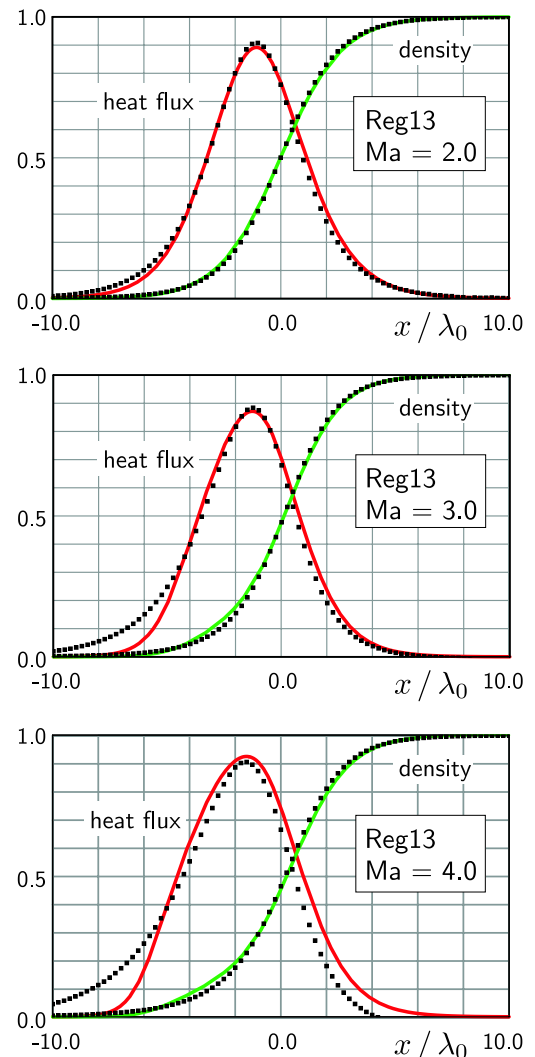

Figure 6. Profiles of density and heat flux inside a shock wave calculated by R13 compared to DSMC (symbols).

small Mach number $Ma \lesssim 3.0$.

One of the main drawbacks of moment equations when proposed by Grad in [8] was the presence of subshocks in shock wave profiles. Fig. 5 shows how the regularization procedure that leads to the R13 equations overcomes this deficiency of Grad's equations. The figure shows the velocity profile of a stationary shock wave with an inflow of $Ma = 3.0$ from the left. The curve of Grad shows a big subshock in the beginning and a smaller one towards the end. The R13 result gives a smooth transition.

For a quantitative test the profiles of R13 have been compared to DSMC results in Fig. 6. The figure shows three stationary shock waves with increasing inflow Mach numbers $Ma = 2.0, 3.0, 4.0$. One curve shows the s-shaped profile of the density,

7

while the other represents the heat flux which is zero before and after the shock wave. Inside the shock wave the strong dissipation results in large values for heat flux, stress, etc. The space scale is given in terms of mean free pathes and indicates the extremely small shock thickness of only 5 to 10 mean free pathes.

The R13 equations match the $Ma = 2.0$ shock wave reasonably well, while for higher Mach numbers the relaxation before the shock is deviating from the DSMC result. Note also, that the density profile is relatively easy to predict, while the heat flux as a higher moment is much harder to match. Details about the shock wave study with R13 can be found in [16].

CONCLUSIONS

With these properties and features, the R13 equations must be considered as the most successful continuum model for gas micro-flows. In contrast to direct simulations or molecular dynamics, such a model gives valuable inside into physical effects by identifying effects inside equations. The application of the R13 equations to a wider variety of micro-flow problems is planned for the future.

REFERENCES

[1] C. Cercignani, *The Boltzmann Equation and its Applications*, Applied Mathematical Sciences 67, Springer, New York, (1988)

[2] H. Struchtrup, *Macroscopic Transport Equations for Rarefied Gas Flows*, Interaction of Mechanics and Mathematics, Springer, New York (2005)

[3] A.V. Bobylev, *The Chapman-Enskog and Grad methods for solving the Boltzmann equation*, Sov. Phys. Dokl. **27**, (1982) p.29-31

[4] A. V. Bobylev, *Instabilities in the Chapman-Enskog Expansion and Hyperbolic Burnett Equations*, J. Stat. Phys. **124** (2-4), (2006), p.371-399

[5] S. Jin and M. Slemrod, *Regularization of the Burnett equations via relaxation*, J. Stat. Phys. **103** (5-6), (2001) p.1009-1033

[6] R. K. Agarwal, K. Y. Yun, and R. Balakrishnan, *Beyond Navier-Stokes: Burnett equations for flows in the continuum-transition regime*, Phys. Fluids **13**, (2001), p.3061-3085, Erratum: Phys. Fluids **14**, (2002), p.1818

[7] D. A. Lockerby and J. M. Reese, *High-resolution Burnett simulations of micro Couette flow and heat transfer*, J. Comput. Phys. **188**(2), (2003), p.333-347

[8] H. Grad, *On the Kinetic Theory of Rarefied Gases*, Comm. Pure Appl. Math. **2**, (1949), p.331-407

[9] W. Weiss, *Continuous shock structure in extended Thermodynamics*, Phys. Rev. E **52**, (1995), p.5760

[10] I. Müller and T. Ruggeri, *Rational Extended Thermodynamics* (2nd edn), Springer Tracts in Natural Philosophy (vol.37), Springer, New York (1998)

[11] J. D. Au, M. Torrilhon, and W. Weiss, *The Shock Tube Study in Extended Thermodynamics*, Phys. Fluids **13**(8) , (2001) p.2423-2432

[12] C. D. Levermore, *Moment closure hierarchies for kinetic theories*, J. Stat. Phys. **83**(5-6), (1996) p.1021-1065

[13] B.-C. Eu, *A Modified Moment Method and Irreversible Thermodynamics*, J. Chemical Phys. **73**(6), (1980) p.2958-2969

[14] R.-S. Myong, *A computational method for Eu's generalized hydrodynamic equations of rarefied and microscale gas dynamics*, J. Comput. Phys. **168**(1), (2001) p.47-72

[15] H. Struchtrup and M. Torrilhon, *Regularization of Grad's 13-Moment-Equations: Derivation and Linear Analysis*, Phys. Fluids **15**/9, (2003), pp.2668-2680

[16] M. Torrilhon and H. Struchtrup, *Regularized 13-Moment-Equations: Shock Structure Calculations and Comparison to Burnett Models*, J. Fluid Mech. **513**, (2004), pp.171-198

[17] H. Struchtrup, *Stable transport equations for rarefied gases at high orders in the Knudsen number*, Phys. Fluids **16**(11), (2004) p.3921-3934

[18] H. Struchtrup, *Derivation of 13 moment equations for rarefied gas flow to second order accuracy for arbitrary interaction potentials*, Multiscale Model. Simul. **3**(1), (2005) p.221-243

[19] I. Müller, D. Reitebuch, and W. Weiss, *Extended Thermodynamics - Consistent in Order of Magnitude*, Cont. Mech. Thermodyn. **15**(2), (2003) p.411-425

[20] X. Gu and D. Emerson, *A Computational Strategy for the Regularized 13 Moment Equations with Enhanced Wall-Boundary Conditions*, J. Comput. Phys. **225** (2007), p.263-283

[21] M. Torrilhon and H. Struchtrup, *Boundary Conditions for Regularized 13-Moment-Equations for Micro-Channels*, J. Comput. Phys., (2007), accepted

[22] H. Struchtrup, *Scaling and expansion of moment equations in kinetic theory*, J. Stat. Phys. **125**, (2006), p.565

[23] J. C. Maxwell, *On Stresses in Rarefied Gases Arising From Inequalities of Temperature*, Phil. Trans. Roy. Soc. (London) **170**, (1879), p.231-256

[24] H. Struchtrup, *Grad's Moment Equations for Microscale Flows*, 23rd Intl. Symposium on Rarefied Gas Dynamics, AIP Proceedings 663, (2003), p.792-799

[25] G. A. Bird, *Molecular Gas Dynamics and the Direct Simulation of Gas Flows* (2nd edn), Oxford University Press, New York (1998)

[26] H. Struchtrup and M. Torrilhon, *H-theorem, regularization, and boundary conditions for linearized 13 moment equations*, Phys. Rev. Letters **99**, (2007) 014502

[27] H. Struchtrup, *Failures of the Burnett and Super-Burnett equations in steady state processes*,

Cont. Mech. Thermodyn. **17**(1), (2005), p.43-50

[28] H. Struchtup and T. Thatcher, *Bulk equations and Knudsen layers for the regularized 13 moment equations*, Cont. Mech. Thermodyn. **19**(3) (2007), p.177-189

[29] M. Torrilhon, *Two-Dimensional Bulk Microflow Simulations Based on Regularized 13-Moment-Equations*, SIAM Multiscale Model. Simul. **5**(3), 695-728 (2006)

[30] M. Torrilhon, *Regularized 13-Moment-Equations*, 25th Intl. Symposium on Rarefied Gas Dynamics, St. Petersburg, Russia, (2006)

[31] Y. Zheng, A. L. Garcia, and J. B. Alder, *Comparison of kinetic theory and hydrodynamics for Poiseuille flow*, J. Stat. Phys. **109**, (2002), p.495-505

[32] K. Xu and Z.-H. Li, *Microchannel flow in the slip regime: gas-kinetic BGK-Burnett solutions*, J. Fluid Mech. 513, (2004) p.87-110

[33] M. Knudsen, *Die Gesetze der Molekularströmung und der inneren Reibungsströmung der Gase durch Röhren*, Ann. Phys. **333**, (1909), p.75-130

[34] T. Ohwada, Y. Sone and K. Aoki, *Numerical analysis of the Poiseuille and thermal transpiration flows between two parallel plates on the basis of the Boltzmann equation for hard-sphere molecules*, Phys. Fluids A **1**(12), (1989), p.2042-2049